## RESEARCH ARTICLE

# Regulation of kinesin-1 activity by the *Salmonella enterica* effectors PipB2 and SifA

Lucrecia Alberdi[1], Alexandra Vergnes[1], Jean-Baptiste Manneville[2,3], Dumizulu L. Tembo[1], Ziyan Fang[1], Yaya Zhao[1], Nina Schroeder[1], Audrey Dumont[1], Margaux Lagier[1], Patricia Bassereau[4,5], Lorena Redondo-Morata[6], Jean-Pierre Gorvel[1] and Stéphane Méresse[1,*]

## ABSTRACT

*Salmonella enterica* is an intracellular bacterial pathogen. The formation of its replication niche, which is composed of a vacuole associated with a network of membrane tubules, depends on the secretion of a set of bacterial effector proteins whose activities deeply modify the functions of the eukaryotic host cell. By recruiting and regulating the activity of the kinesin-1 molecular motor, *Salmonella* effectors PipB2 and SifA play an essential role in the formation of the bacterial compartments. In particular, they allow the formation of tubules from the vacuole and their extension along the microtubule cytoskeleton, and thus promote membrane exchanges and nutrient supply. We have developed *in vitro* and *in cellulo* assays to better understand the specific role played by these two effectors in the recruitment and regulation of kinesin-1. Our results reveal a specific interaction between the two effectors and indicate that, contrary to what studies on infected cells suggested, interaction with PipB2 is sufficient to relieve the autoinhibition of kinesin-1. Finally, they suggest the involvement of other *Salmonella* effectors in the control of the activity of this molecular motor.

This article has an associated First Person interview with the first author of the paper.

KEY WORDS: Effector protein, Infection, Kinesin-1, PipB2, *Salmonella*, SifA, Membrane tubules

## INTRODUCTION

The species *Salmonella enterica* is composed of a large number of serotypes, including typhoid strains, which cause severe systemic disease (typhoid fever) in humans, and non-typhoid strains responsible for acute gastroenteritis. The latter may also cause systemic infection in hosts already weakened by another viral or parasitic infection (Gordon et al., 2008). The non-typhoid strain S. Typhimurium (*Salmonella enterica* subsp. *enterica* serotype

[1]Aix-Marseille Université, CNRS, INSERM, CIML, Marseille, France. [2]Institut Curie, PSL Research University, CNRS, UMR 144, 26 rue d'Ulm, F-75005, Paris, France. [3]Sorbonne Université, UPMC University Paris 06, CNRS, UMR 144, 26 rue d'Ulm, F-75005, Paris, France. [4]Laboratoire Physico Chimie Curie, Institut Curie, PSL Research University, CNRS UMR168, 75005 Paris, France. [5]Sorbonne Université, 1 Place Jussieu, 75005 Paris, France. [6]U1006 INSERM, Aix-Marseille Université, Marseille, France.

*Author for correspondence (meresse@ciml.univ-mrs.fr)

L.A., 0000-0001-9421-3311; A.V., 0000-0001-6745-6633; J.-B.M., 0000-0002-8670-3940; D.L.T., 0000-0002-7604-1752; Y.Z., 0000-0001-6424-8687; N.S., 0000-0003-4905-1805; A.D., 0000-0001-6043-7237; M.L., 0000-0002-8823-8560; P.B., 0000-0002-8544-6778; L.R., 0000-0002-6254-8261; J.-P.G., 0000-0002-2829-9804; S.M., 0000-0001-6578-5177

Typhimurium) is commonly used as a model for studying host-pathogen interactions (LaRock et al., 2015).

*Salmonella* is an enteropathogenic bacterium. During the infectious process, bacteria that have reached the gut cross the intestinal barrier, preferably through the M cells of Peyer's patches (Lelouard et al., 2012) and to a lesser extent by infecting enterocytes. They then migrate and are found in a multitude of cell types, especially in cells of the immune system (Aussel et al., 2011), in Peyer's patches, in liver, in spleen and also in epithelial cells, e.g. the gallbladder (Knodler et al., 2010).

The pathogenicity of *Salmonella* depends on its ability to replicate intracellularly in a membrane-bound compartment called the *Salmonella*-containing vacuole (SCV). The membrane of the SCV is enriched with lysosomal proteins. Infected cells show a rarefaction of lysosomal vesicles that seem to have merged with the SCVs. This recruitment of lysosomal membranes takes place thanks to the formation of membrane tubules that are formed from the SCVs and extend on the network of microtubules in the cells. These tubular membrane structures, called *Salmonella*-induced tubules, promote exchange with lysosomal vesicles, membrane recruitment and transport of material to the SCVs (Liss et al., 2017), and ultimately provide the nutrients necessary for intracellular bacterial replication (Noster et al., 2019).

This unique process is orchestrated by a series of bacterial proteins that are injected into the host cell cytosol by a type III secretion system (T3SS), which is encoded by the second pathogenicity island (T3SS-2). The T3SS-2 effector proteins influence a large number of cellular processes, such as gene expression (Mazurkiewicz et al., 2008), localization of membrane proteins (Bayer-Santos et al., 2016) or dynamics of the cytoskeleton (Abrahams et al., 2006; Méresse et al., 2001). By interacting with the microtubule motor protein kinesin-1, the two effector proteins PipB2 (Henry et al., 2006) and SifA (Boucrot et al., 2005) play a particularly important role in the formation and function of *Salmonella*-induced tubules. Kinesin-1 is a hetero-tetrameric ATPase composed of two heavy chains (KHCs; KIF5A–KIF5C) and two light chains (KLCs; KLC1–KLC4) that promotes the transport of cargoes toward the growing end of microtubules. PipB2 interacts directly with KLCs (Henry et al., 2006), while SifA binds to SKIP (also known as PLEKHM2), an adaptor host protein that interacts with KLCs (Boucrot et al., 2005; Dumont et al., 2010).

In the absence of cargo binding, kinesin-1 adopts a folded, compact conformation that is auto-inhibited and cytosolic (Cai et al., 2007). Cargo binding relieves autoinhibition and results in an extended structure, releasing KHC motor domains that engage with the microtubules (Hirokawa and Noda, 2008) and convert the chemical energy of ATP hydrolysis into motion along microtubules. The mechanism of activation of kinesin-1 is not yet fully understood. It involves interactions between the cargo and both

KHCs and KLCs, the latter being involved in the inhibition of the enzymatic activity of the KHCs. In the cellular context, binding of the cargo protein JIP1 (also known as MAPK8IP1) to KLCs is not sufficient to activate kinesin-1 and requires additional interactions of KHCs with FEZ1 (Blasius et al., 2007). The TPR domain of KLC recognizes a peptide sequence composed of a tryptophan (Dodding et al., 2011) or a tyrosine (Pernigo et al., 2018) residue flanked by acid residues, sequences that have recently been named W-acidic and Y-acidic. The W-acidic motif originally characterized in vaccinia virus protein A36 is also found in many adaptor proteins such as SKIP, which contains two of them (Pernigo et al., 2013). A recent study showed that SKIP can also interact with KHCs when already interacting with KLCs, and that this double interaction relieves the auto-inhibition of kinesin-1 (Sanger et al., 2017).

In *Salmonella*-infected cells, SifA and PipB2 are important for the formation and/or elongation of *Salmonella*-induced tubules. Cells infected with a mutant Δ*pipB2* are characterized by the formation of short tubules (Knodler and Steele-Mortimer, 2005), whereas these are lacking or very rare in the absence of SifA (Stein et al., 1996) or SKIP (Boucrot et al., 2005). The specific impact of PipB2 and SifA on kinesin-1 activation is still not understood. However, based on previous observations and, in particular, because PipB2-bound kinesin-1 accumulates on SCVs in the absence of SifA, we proposed that the SifA/SKIP complex is necessary for the activation of the kinesin-1 recruited by PipB2 (Dumont et al., 2010; Leone and Méresse, 2011). In this study, we have used *in vitro* and *in cellulo* approaches to investigate the activation status of kinesin-1 when recruited by PipB2 and SifA effectors.

## RESULTS
### Kinesin-1 is important for membrane dynamics and intracellular positioning of SCVs
To better understand the role played by kinesin-1 in the formation of vesicles and tubules emerging from SCVs, we analysed the consequences of the absence of the molecular motor in *Salmonella*-infected cells. For this purpose, we differentiated macrophages from Hoxb8-immortalized macrophage-committed progenitor cells (Redecke et al., 2013; Wang et al., 2006). These cells were derived from C57BL/6 mice expressing KIF5B (kinesin-1 heavy chain) in hematopoietic cells or not (Munoz et al., 2016). By western blotting, anti-KHC antibody recognized a band between 100 and 150 kDa in KIF5B$^{+/+}$ macrophages and mouse brain cytosol that was absent in KIF5B$^{-/-}$ macrophages (Fig. 1A), thus confirming the absence of functional kinesin-1.

The macrophages were infected with a *S.* Typhimurium strain (wild-type) expressing GFP and a HA-tagged version of the T3SS-2 effector protein SseJ and observed by confocal microscopy 14 h after infection. GFP was used to detect the presence of bacteria in cells. LAMP1 and SseJ were used as membrane markers of bacterial compartments. While *Salmonella*-induced tubules form in most infected epithelial cells, these membrane structures are only rarely seen in non-activated macrophages (Knodler et al., 2003; Krieger et al., 2014). In macrophages, effectors tend to be located on discrete vesicles throughout the cell (Freeman et al., 2003; Ohlson et al., 2005). Unsurprisingly, in KIF5B$^{+/+}$ macrophages infected with wild-type *Salmonella*, SseJ was present on SCVs and also at distance from SCVs in association with vesicular structures (Fig. 1B). In contrast, SseJ was essentially localized on SCVs in the absence of kinesin-1 and also in KIF5B$^{+/+}$ cells infected with the Δ*sifA* mutant (Fig. 1B,C) as expected (Zhao et al., 2015). These results indicate that kinesin-1 is required for the mechanisms by which SseJ traffics from SCVs to discrete vesicular structures. They also support the

previously proposed hypothesis (Dumont et al., 2010) that associates the absence of vesicles/tubules in cells infected by a Δ*sifA* mutant with a low level of activation of kinesin-1 that, when recruited by PipB2, accumulates on SCVs (Henry et al., 2006).

We also observed an influence of kinesin-1 on the position of SCVs. Whereas in the KIF5B$^{+/+}$ and KIF5B$^{-/-}$ macrophages, the wild-type SCVs were located in the juxtanuclear region (Fig. 1C), they were grouped very compactly and close to the nucleus in the absence of kinesin-1 (Fig. 1B). This indicates that kinesin-1 has an anterograde transport activity that maintains the SCVs in the juxtanuclear region but at some distance from the nucleus. In KIF5B$^{+/+}$ macrophages, two populations of Δ*sifA* SCVs were distinguished according to whether or not they were positive for SseJ. The positive ones, which are also those that accumulate kinesin-1 (Zhao et al., 2015), showed a localization much further from the nucleus than other vacuoles. This difference was not found in the KIF5B$^{-/-}$ macrophages where vacuoles indistinctly adopt a juxtanuclear position (Fig. 1B,C), and shows that the kinesin-1 present on Δ*sifA* SCVs, although not very active, is nevertheless responsible for the anterograde movement of bacterial vacuoles. Overall, these results underline the importance of kinesin-1 in the formation of effector-positive membrane vesicles derived from SCVs, indicating that this molecular motor is also necessary for the anterograde movement of SCVs and confirming the low state of activation of PipB2-bound kinesin-1 present on Δ*sifA* SCVs.

### PipB2-bound kinesin-1 is active
PipB2 plays a key role in the recruitment of kinesin-1 on SCVs (Boucrot et al., 2005; Henry et al., 2006). However, it is still unknown whether kinesin-1 is the only molecular motor recruited by PipB2 and whether this effector can distinguish between the activation states of kinesin-1 or play a role in the activation of this molecular motor. To gain insights on the motor activity of PipB2-bound proteins, we reconstituted an *in vitro* microtubule gliding assay. It consists of a streptavidin-coated glass chamber successively filled with biotinylated Δ17PipB2 (Bio-PipB2), a fraction of molecular motors, fluorescent microtubules and a motility buffer containing 1 mM ATP (Fig. S1A). As a positive control, the glass chamber was coated with the biotinylated motor domain of *Drosophila* kinesin heavy chain (K401-Bio). This constitutively active recombinant protein (Roux et al., 2002; Subramanian and Gelles, 2007) induced a microtubule gliding with a velocity of 0.05±0.01 μm/s and a narrow distribution of gliding velocities (Fig. 2; Fig. S2A and Movie 1). In the presence of Bio-PipB2 and MAP-depleted mouse brain cytosol as a source of molecular motors, we observed persistent attachment and sustained movement of the microtubules after injection of motility buffer (Fig. 2; Fig. S2B,C). The microtubules displayed a gliding motility throughout the recorded period of 15 min (Movie 2) with a velocity of 0.22±0.01 μm/s (Fig. S2A), which is higher than that observed with the motor domain of *Drosophila* KHC but inferior to the gliding speed of 0.5-0.7 μm/s reported in the literature in a similar assay using bovine kinesin (Grummt et al., 1998). When biotinylated BSA (Bio-BSA), our negative control, was injected instead of PipB2, we noticed the gliding of a small fraction of microtubules (Fig. 2; Fig. S2C) and the rapid decrease in the number of attached microtubules (Fig. S2B, Movie 3). We concluded that the attachment and the movement of the microtubules depend on PipB2.

To determine whether kinesin-1 is the cytosolic factor mediating microtubule gliding, we fractionated a cytosol preparation enriched in microtubule-based motors by centrifugation on a sucrose gradient. Fraction 7, which presented the highest concentration of
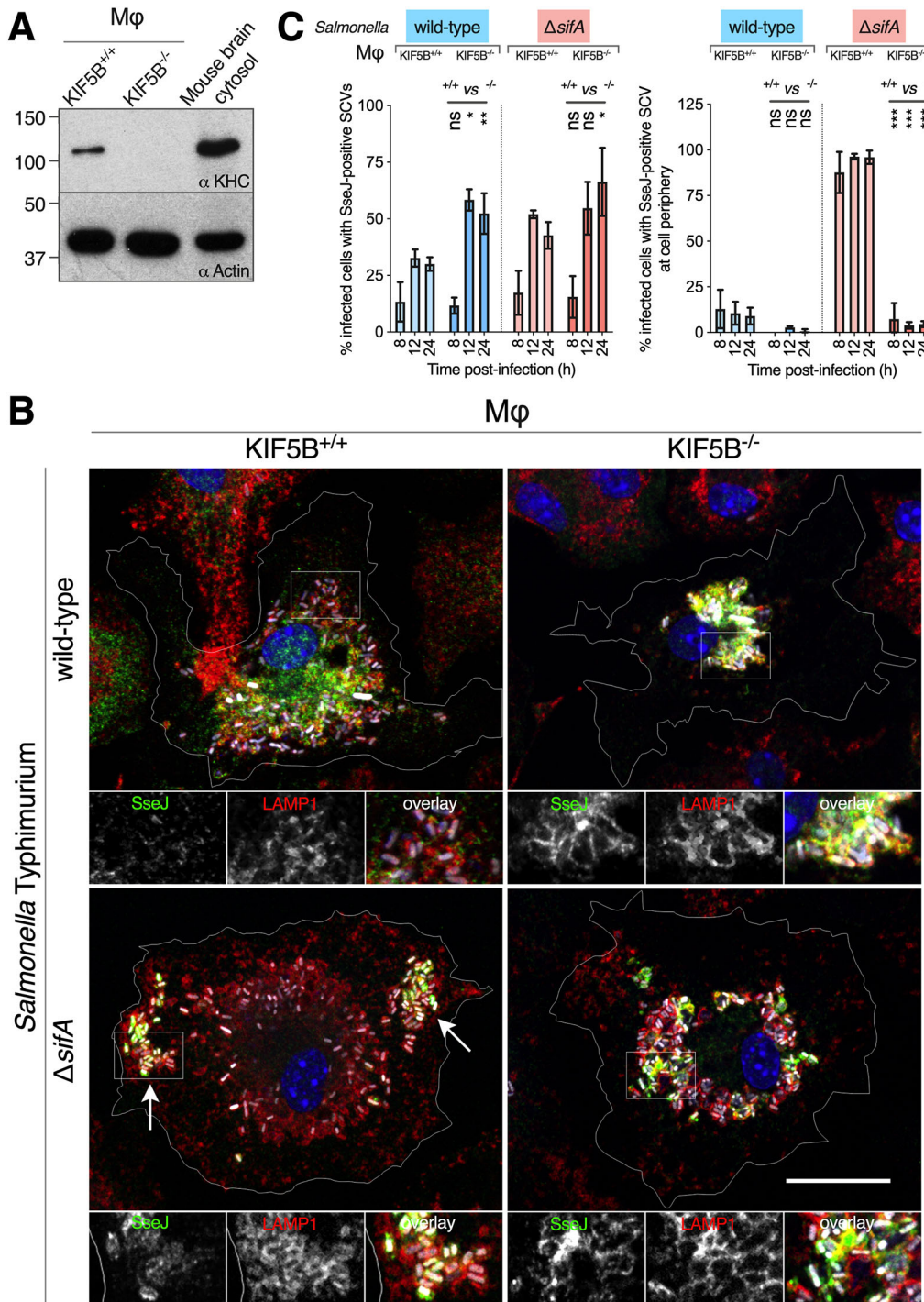
Fig. 1. Impact of the absence of kinesin-1 in *Salmonella*-infected macrophages. (A) Kinesin heavy chain is not detected in KIF5B⁻/⁻ Hoxb8 macrophages. Western blotting showing KHC expression in cell lysates of wild-type (KIF5B⁺/⁺) or KIF5B⁻/⁻ Hoxb8 macrophages and mouse brain cytosol. Actin was used as loading control. (B,C) KIF5B⁺/⁺ and KIF5B⁻/⁻ Hoxb8 macrophages (Mφ) were infected with wild-type or Δ*sifA* strains of *S.* Typhimurium expressing GFP from a plasmid and SseJ-2HA from the chromosome. Cells were fixed at different times post-infection and immunostained for LAMP1 and HA. (B) Cells (14 h post-infection) were imaged by confocal microscopy for LAMP1 (red), SseJ (green), *Salmonella* (white) and nuclei (blue). Magnifications of the boxed areas showing single labelling are presented below each image. In the absence of functional kinesin-1, wild-type SCVs form a compact cluster very close to the nucleus, while SseJ-positive Δ*sifA* SCVs which, in KIF5B⁺/⁺ macrophages are at the periphery (arrows), are located in the juxtanuclear area. Scale bar: 20 µm; 10 µm in insets. (C) Percentages of infected cells with SseJ-positive SCVs (left graph) or SseJ-positive SCVs located at the cell periphery (right graph). Phenotypes were scored at three infection times. SCVs were counted as positive for SseJ when the labelling for this effector identified the vacuolar compartment enclosing the bacteria and considered to be peripheral when they were in the outer one-third of the cytoplasmic space. Data are mean±s.d. of three independent experiments. A two-way ANOVA was used to compare the results obtained in cells expressing or not expressing KIF5B at each time after infection and for each bacterial strain. ns, $P>0.05$; *$P<0.05$; **$P<0.01$; ***$P<0.001$.

kinesin-1 (Fig. S3A) was tested in the gliding assay. We observed a velocity of 0.15±0.01 µm/s, of the same order of magnitude as that obtained with MAP-depleted mouse brain cytosol (Fig. 2; Fig. S2A and Movie 4). To confirm the involvement of kinesin-1 in the PipB2-mediated motility, we prepared cytosol fractions from Hoxb8 macrophages. KIF5B⁺/⁺ cytosol promoted the gliding of microtubules with a speed of 0.23±0.02 µm/s (Fig. 2; Fig. S2A and Movie 5). In the presence of KIF5B⁻/⁻ cytosol, a small fraction of microtubules that partially attached sometimes showed random mobility over a short period before detaching (Fig. 2; Fig. S2C, S2D and Movie 6). Overall, these results indicate that kinesin-1 is responsible for the gliding of microtubules observed in this assay and

that PipB2-bound kinesin-1 is capable of engaging microtubules and inducing their movement in the presence of ATP.

## PipB2-bound kinesin-1 is sufficient to pull tubules from giant unilamellar vesicles

The formation of *Salmonella*-induced tubules from SCVs requires an intact microtubule network where tubules exhibit a bidirectional movement (Drecktrah et al., 2008; Krieger et al., 2014; Rajashekar et al., 2008). Using a minimal biomimetic membrane system *in vitro*, we tested whether the PipB2/kinesin-1 complex could provide enough force to generate membrane tubule networks from giant unilamellar vesicles (GUVs). GUVs were made fluorescent by
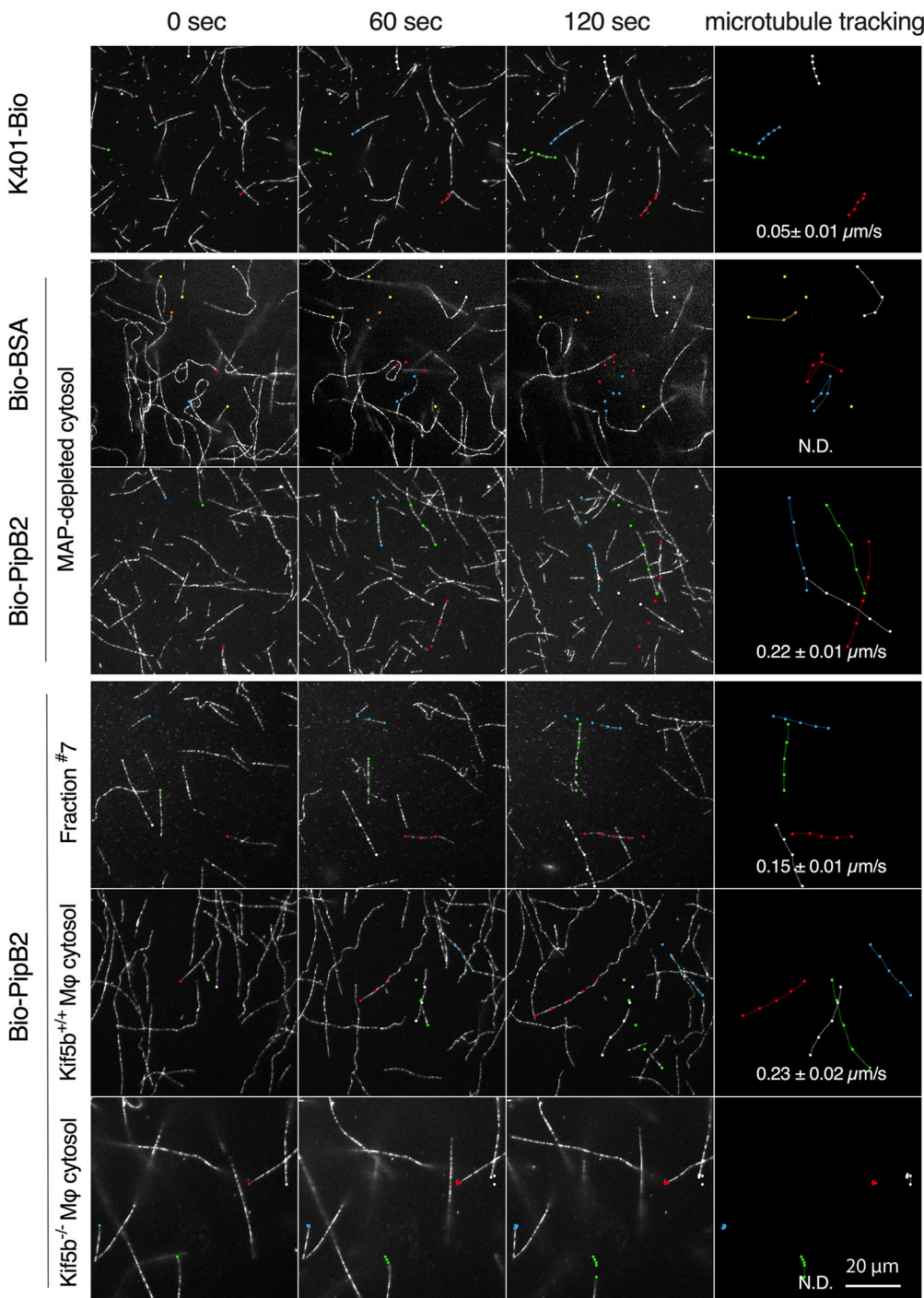
**Fig. 2. PipB2-bound kinesin-1 is capable of gliding microtubules *in vitro*.** As positive control, the chamber was coated with the motor domain of kinesin-1 (K401-Bio, top row). Otherwise, glass chambers were coated with BSA (Bio-BSA, negative control) or PipB2 (Bio-PipB2) and filled with MAP-depleted mouse brain cytosol fraction 7 (which was enriched with microtubule-based motor proteins) or with cytosol prepared from KIF5B$^{+/+}$ or KIF5B$^{-/-}$ Hoxb8 macrophages. Subsequently, rhodamine microtubules and motility buffer containing ATP were injected. Microtubule gilding was observed at 30 s intervals for periods ranging from 2 to 30 min. Each image shows, for each condition, the tracking of four microtubules over a 2 min period at 0, 60 and 120 s. To facilitate the visualization of the movement, the minus end of these microtubules has been marked with a coloured dot and its positions at times 0, 30, 60, 90 and 120 s are indicated in the last column. A rapid detachment of the microtubules was observed in the absence of PipB2 (Bio-BSA) (orange tracks and yellow dots for the last detected point). The mean speed±s.d. of movement of the microtubules is indicated in the last column. Scale bar: 20 μm. Experimental repeats: K401-Bio, *n*>9; MAP-depleted cytosol+Bio-BSA, *n*=3; MAP-depleted cytosol+Bio-PipB2, *n*>15; Fraction 7+Bio-PipB2, *n*>6; KIF5B$^{+/+}$ macrophage cytosol+Bio-PipB2, *n*>3; KIF5B$^{-/-}$ macrophage cytosol+Bio-PipB2, *n*>3. Independent preparations: K401-Bio, *n*=2; MAP-depleted cytosol, *n*=3; Bio-PipB2, *n*=2; Fraction 7, *n*=2; KIF5B$^{+/+}$ macrophage cytosol, *n*=1; KIF5B$^{-/-}$ macrophage cytosol, *n*=1.

addition of 1% β-BODIPY-DOPC and contained 0.1% biotinylated-DOPE, making them capable of binding biotinylated proteins in the presence of streptavidin (Fig. 3A). We modified the tube pulling assay previously described (Leduc et al., 2004). Briefly, in a flow chamber covered by fluorescent microtubules, we sequentially injected the biotinylated protein in the presence of streptavidin, a motility buffer containing 1 mM ATP and GUVs (Fig. S1B). We used K401-Bio and Bio-BSA as positive and negative controls, respectively. In the presence of K401-Bio, we observed the formation of an extended network of tubules, pulled from the GUVs, which extended along the microtubules network (Fig. S4), whereas no tubule was observed with Bio-BSA (Fig. 3B).

These results validated the experimental system. When using Bio-PipB2 pre-incubated with a kinesin-1-containing fraction, we obtained networks of tubules similar to those observed with K401-Bio (Fig. 3B). Taken together, these results confirm that PipB2-bound kinesin-1 is capable of engaging microtubules and demonstrate that the force produced by the complex is sufficient to induce membrane tubules.

## PipB2 increases the activation state of kinesin-1

The vast majority of cellular kinesin-1 is cytosolic and inactive in a folded state that blocks its interaction with microtubules (Cai et al., 2007). Yet our results indicate that at least a part of PipB2-bound

kinesin-1 is active. This can be due to the presence of a significant fraction of active kinesin-1 in the mouse cytosol and the capacity of PipB2 to indifferently bind active or auto-inhibited kinesin-1. Another possibility is the capacity of PipB2 to relieve the autoinhibition of the microtubule motor. To discriminate between these hypotheses, we developed a microtubule-binding protein spin-down assay to evaluate the fraction of cytosolic kinesin-1 that is capable of engaging microtubules (activated kinesin-1) in the presence or absence of PipB2. Briefly, *in vitro* polymerized microtubules were incubated with the proteins of interest and sedimented through a glycerol cushion by ultracentrifugation. As a control, incubations were performed in the absence of polymerized microtubules.

We first analysed by SDS-PAGE and western blotting the distribution of K401-Bio in the supernatant and pellet fractions. This recombinant protein is constitutively active (Roux et al., 2002; Subramanian and Gelles, 2007). The presence of microtubules significantly increased the proportion of the motor domain in the pellet (∼40% compared to ∼10% in the absence of microtubules) (Fig. 4A). This result indicates that K401-Bio is capable of engaging microtubules but remains in the supernatant in the absence of microtubules. Next, we analysed the consequences of introducing Bio-PipB2 on the activation of kinesin-1 in a mouse brain cytosolic fraction. In the absence of microtubules, kinesin-1 was not detectable in the pellet, whether or not PipB2 was present (Fig. 4B). In the presence of microtubules, ∼40% of total kinesin-1 was found in the pellet. This fraction was increased to 90% in the presence of PipB2 (Fig. 4B), which was also present in greater quantity in the pellet in the presence of microtubules (Fig. 4C). We performed a dose-response experiment and observed a correlation between the amount of PipB2 added and kinesin-1 present in the pellet (Fig. 4D). These results indicate that PipB2 activates kinesin-1 and increases the fraction of molecular motor that engages microtubules.

## PipB2 and SifA interact directly

As both PipB2 and SifA interact with kinesin-1 and influence, as the above results show for PipB2, or may influence (SifA; Schroeder et al., 2011) the activity of kinesin-1, we considered the possibility of an interaction between SifA and PipB2. HeLa cells were transfected with plasmids for the expression of GFP or GFP-tagged PipB2 and Myc-tagged variants of SifA. We used cell lysates to immunoprecipitate GFP proteins and analysed the associated proteins by SDS-PAGE and anti-Myc western blotting. SifA co-immunoprecipitated with GFP-PipB2 but not with GFP (Fig. 5A), indicating a specific interaction between the two effectors. We tested the two SifA domains (Ohlson et al., 2008) and found an interaction of PipB2 with the N-terminal part of SifA (Fig. 5A). Finally, we expressed and purified GST-PipB2 and [His]$_6$-SifA from *E.* coli and performed a GST pull-down assay to assess whether or not the interaction is direct. We used raw or GST-coated beads as controls for the specificity and the TPR domain of mouse KLC2 (His$_6$-KLC) as a positive control for the interaction with GST-PipB2. Results indicate a specific direct interaction between SifA and PipB2 (Fig. 5B).

## SifA and PipB2 do not influence their respective activities

We checked whether SifA alone or in combination with PipB2 and in the presence of cytosol (a source of kinesin-1 and SKIP) could bind and influence the activity state of the molecular motor. As the gliding and tubulation assays used a form of PipB2 with its first 17 amino acid residues deleted (Bio-PipB2), we verified that this
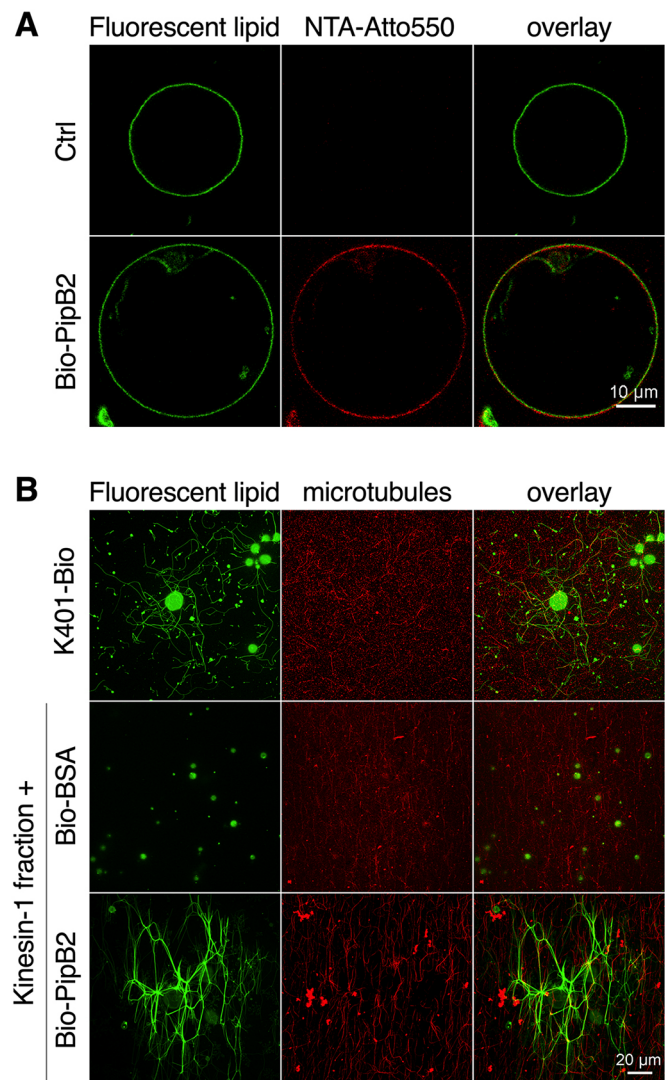


**Fig. 3. PipB2-bound kinesin-1 is capable of pulling membranous tubules from GUVs *in vitro*.** (A) Representative confocal images of GUVs at the equatorial plane. GUVs were made fluorescent by the presence of BodipyFL-C5-HPC (green) in their composition and incubated in the presence or absence of Bio-PipB2. The presence of Bio-PipB2 on the surface of the GUV was revealed by the addition of NTA-Atto 550 (red), which binds the [His]6 tag of the effector. Scale bar: 10 µm. (B) Membranous tubules are pulled from GUVs in the presence of PipB2 and cytosol. GUVs were coated with K401-Bio or with Bio-BSA/Bio-PipB2 in the presence of fraction 7 enriched with microtubule-based motor proteins and injected into the chamber coated with microtubules. K401-Bio and Bio-BSA were used as positive and negative controls, respectively. Confocal fluorescence images for the GUV membrane (green) and microtubules (red) were taken in the microtubule plane. Long membrane tubules following microtubule tracks were induced by K401-Bio and fraction 7 in the presence of Bio-PipB2 but not in the presence of Bio-BSA. Scale bar: 20 µm. Experimental repeats: K401-Bio, *n*>9; Fraction 7+Bio-BSA, *n*=3; Fraction 7+Bio-PipB2, *n*=3. Independent preparations: K401-Bio, *n*=2; Bio-PipB2, *n*=2; Fraction 7, *n*=2.

domain is not necessary for interaction with SifA (Fig. 5A). We then tested the ability of SifA to interact with kinesin-1 or to influence the interaction between the molecular motor and PipB2. For this, streptavidin beads were coupled with Bio-PipB2, SifA-Bio or an equimolar mixture of both effectors and incubated in the presence of cytosol. Bead-bound kinesin-1 was analysed by western blotting using an antibody directed against the KHCs (Fig. S3B). Kinesin-1
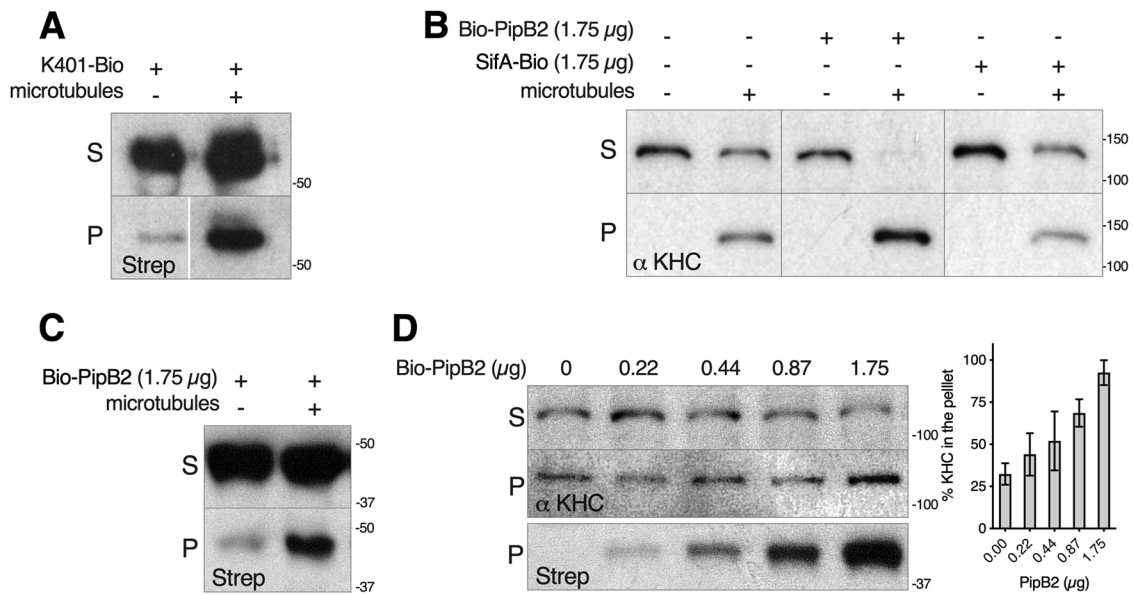
**Fig. 4. PipB2 increases the activation level of kinesin-1.** A microtubule spin-down assay was used to assess changes in the activation level of kinesin-1. Microtubules were incubated with K401-Bio (A) or with MAP-depleted mouse brain cytosol (B-D) supplemented with or without Bio-PipB2 or SifA-Bio. Samples were ultra-centrifuged on glycerol cushions and the supernatants (S) and pellets (P) were analysed by western blotting for the presence of biotinylated proteins (Strep) or KHC. (D) Increasing amounts of PipB2 were added. Protein bands of western blots were quantified using Image J and the fraction of KHC present in pellets was determined. The mean value±s.e.m. of three independent experiments were plotted.

was present on beads coated with PipB2 but not on those coated with SifA. Furthermore, the presence of these two effectors did not influence the recruitment of kinesin-1 in any way. In the microtubule gliding assay, SifA-Bio induced the binding of a low number of microtubules that quickly detached (Fig. S3C and Movie 7). When mixed in an equimolar amount to PipB2, SifA did not modify the PipB2-induced microtubule binding and gliding (Fig. S3C). In the microtubule-binding protein spin-down assay, SifA-Bio did not increase the pelleted fraction of kinesin-1 (Fig. 4B). The conclusion of these experiments is that, under the experimental conditions used, SifA is not capable of changing the activation state of kinesin-1 or of modulating the ability of PipB2 to activate kinesin-1.

### PipB2 activates kinesin-1 *in cellulo*
So far, our results indicate that PipB2 is able to increase the activity of kinesin-1 *in vitro*. We therefore checked whether the same was true in the cellular context. For this, we transfected COS-7 cells with plasmids for the expression of GFP-tagged *Salmonella* effectors and HA-tagged light (mouse KLC2) and heavy (rat KIF5C) chains of kinesin-1. After 24 h we analysed by fluorescence microscopy the impact of *Salmonella* effectors on the activation of the molecular motor, i.e. its presence in the cytosol versus on microtubules. Overexpressed KHC, KLC and kinesin-1 (KHC/KLC) were essentially cytosolic. KHC was also occasionally detected on microtubules (Fig. S5). In agreement with previous studies (Henry et al., 2006; Knodler and Steele-Mortimer, 2005), PipB2 was found in the cytosol and on vesicles on which KLCs, which interact with PipB2, were detected, unlike KHCs (Fig. 6A, upper row). Compared with PipB (a homologue of PipB2; Knodler et al., 2003), we observed a dramatic change in the localization of kinesin-1 in cells expressing PipB2, which then adopted a fibrous appearance and colocalized with microtubules (Fig. 6A, middle row). The fraction of cells in which we detected the presence of kinesin-1 on microtubules increases from 2% to about 65% in the

presence of PipB2, whereas no impact could be observed in cells expressing PipB. In cells expressing KLC we also noted a significant increase of the association with microtubules in the presence of PipB2 (0 versus 20%). This likely reflects the ability of exogenous KLC2 to form functional hybrid molecular motor with endogenous KHC. Finally, we also analysed the impact of SifA in combination with or without PipB2. As seen *in vitro*, the expression of SifA had no impact on the localization of kinesin-1 or on the ability of PipB2 to promote the engagement of kinesin-1 on microtubules (Fig. 6A,B; Fig. S5).

In order to validate these microscopic observations, we biochemically analysed the activation of kinesin-1 in the cellular context as recently described (Sanger et al., 2017). To do this, we lysed the transfected cells under microtubule-stabilizing conditions, centrifuged the lysates and studied the distribution of ectopically expressed proteins in the supernatant and microtubule pellet. To validate the experimental system, we expressed an ATPase 'rigor' mutant of KHC (KHC-R) that associates very stably with microtubules (Guardia et al., 2016) and that was found almost exclusively associated with microtubules in the pellet (Fig. 7). Compared with GFP or PipB, our negative controls, we found that the expression of PipB2 significantly increased the fraction of kinesin-1 associated with microtubules, as was also the case with SKIP, our positive control (Sanger et al., 2017) (Fig. 7). These results confirm the microscopic observations and indicate that, as seen *in vitro*, PipB2 promotes the activation of kinesin-1 in this cellular context.

### DISCUSSION
Here, we show that the interaction between the T3SS-2 effector PipB2 and the KLCs leads to the activation of kinesin-1. This is demonstrated *in vitro* by the activity of PipB2-recruited kinesin-1 in microtubule gliding and GUV tubulation assays, by the ability of PipB2 to increase the fraction of kinesin-1 bound to microtubules, and by the re-localization of kinesin-1 from the cytosol to the microtubule cytoskeleton in cells expressing PipB2.
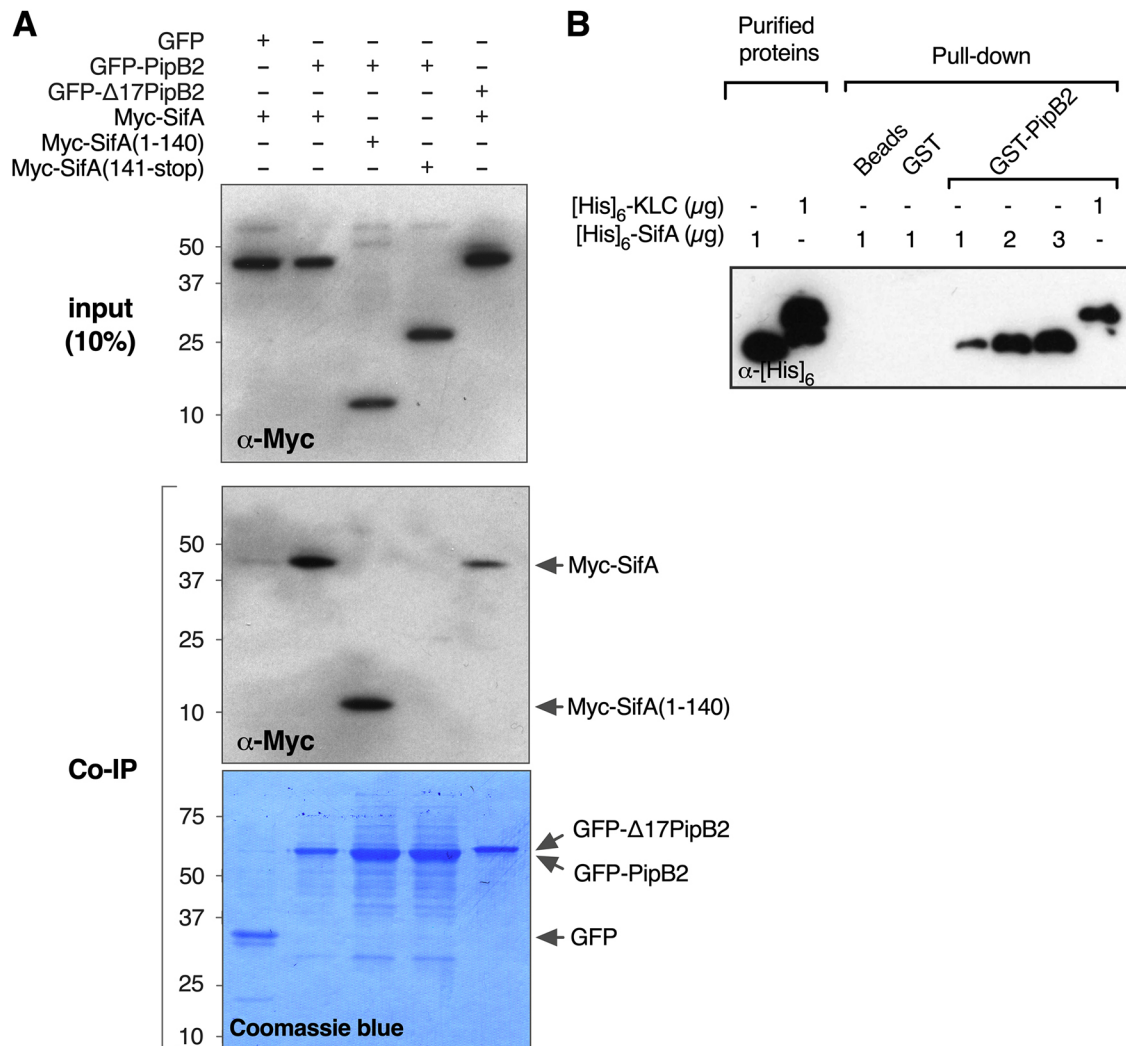
**Fig. 5. PipB2 interacts with SifA.** (A) PipB2 interacts with the N-terminal domain of SifA. HeLa cells were transfected with plasmids for the ectopic expression of GFP or variants of GFP-PipB2 and Myc-SifA. Immunoprecipitations were performed with GFP-Trap beads. Input (top panel) and bound proteins (middle panel) were analysed by western blotting using anti-Myc. Coomassie Blue staining of the PVDF membrane after western blotting is presented (bottom panel). Despite the removal of the N-terminal end, Δ17PipB2 has a higher apparent molecular weight than PipB2. This is due to cloning in the Gateway system and the presence of a large linker between the GFP tag and PipB2 (see Table S2). (B) PipB2 and SifA interact directly. [His]$_6$-SifA or [His]$_6$-KLC (positive control) were incubated with GST or GST-PipB2 immobilized on glutathione beads. Purified and pulled-down proteins were analysed by western blotting with an anti-[His]$_6$ antibody.

Kinesin-1 mainly exists in a folded conformation that is auto-inhibited, i.e. inactive for microtubule-based motility (Cai et al., 2007). Several examples show that the interaction of KLCs with cargo participates in the activation of the molecular motor (Blasius et al., 2007; Cai et al., 2007; Sanger et al., 2017). From this point of view, the results obtained with PipB2 are not surprising. However, they are not consistent with observations made in the infectious context. Previous studies have shown that by recruiting kinesin-1 to the SCV, PipB2 induces elongation of tubules emerging from bacterial vacuoles. However, in the absence of SifA, these tubules/vesicles do not form and a PipB2-dependent accumulation of kinesin-1 is observed on SCVs. Based on these observations, we proposed (Boucrot et al., 2005) that: (1) the kinesin-1 present on Δ*sifA* SCVs is weakly or not active, which prevents the formation of tubules/vesicles from SCVs; (2) the SifA/SKIP complex is necessary for the activation of the kinesin-1 recruited by PipB2. This model is supported by a recent study (Sanger et al., 2017) demonstrating that multiple interactions of the N-terminal part of SKIP with KLC and KHC promote activation of kinesin-1. The data

presented here also support this model as they show that the absence of functional kinesin-1 in macrophages is associated with the presence of SseJ on SCVs, a phenotype seen in the absence of SifA. This strongly suggests that the kinesin-1 recruited by PipB2 on Δ*sifA* SCVs is essentially inactive.

Our results thus show that the control of the activity of the kinesin-1 present on SCV is more complex than initially thought and suggest the involvement of other *Salmonella* effectors and/or host proteins. Among the effectors (other than SifA and PipB2) known to influence vesicle/tubule formation, two have activities compatible with possible involvement in the regulation of kinesin-1. Although not essential for the formation of *Salmonella*-induced tubules, SseJ promotes the tubulation of the lysosomal compartment when expressed ectopically with SifA (Ohlson et al., 2008). This event depends on SKIP and microtubules, which suggests that SseJ exacerbates the ability of SifA to induce tubulation (Boucrot et al., 2003) and reveals a functional interaction that is important for the formation of tubules. SopD2, when inactivated together with SifA, results in a strain (Δ*sifA*Δ*sopD2*) that produces tubules. This
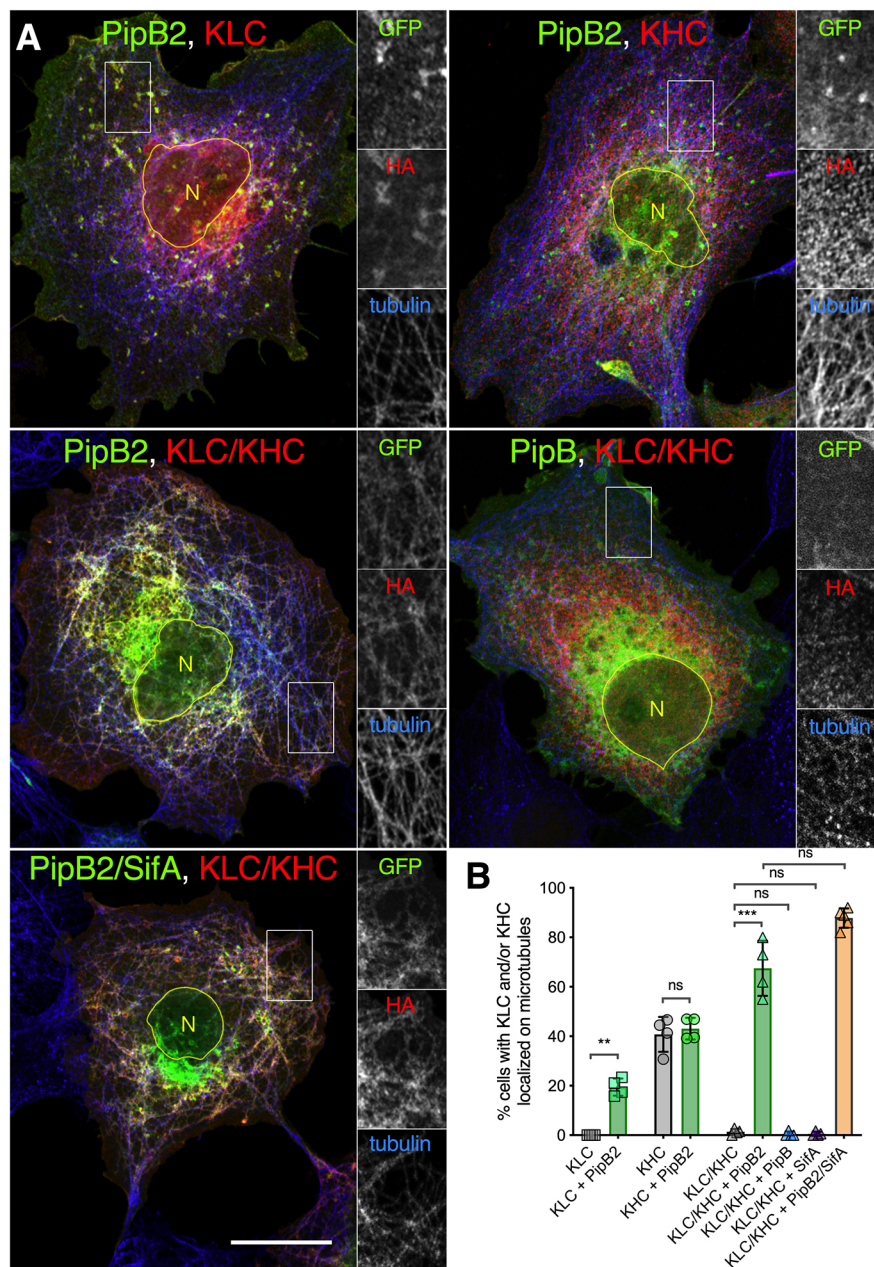
**Fig. 6. PipB2 re-localizes kinesin-1 onto microtubules.** COS-7 cells were transfected with plasmids for the ectopic expression of HA-tagged KLC or KHC, or KLC and KHC (kinesin-1) and of a GFP-tagged effector (PipB2, SifA or PipB). (A) Fixed cells were immunostained and imaged by confocal microscopy for GFP (green), HA (red) and tubulin (blue). For the cells of interest, a yellow line outlines the position of the nuclei (N). Insets show magnifications of the areas in rectangles with single labelling. Scale bar: 20 μm; 10 μm (insets). (B) The presence of HA labelling on microtubules was scored. Only transfected cells expressing both GFP- and HA-tagged proteins were considered. Values are mean±s.d. of at least three independent experiments. For statistical analysis, paired *t*-tests were used to compare the means. ns, not significant; \*\**P*<0.01; \*\*\**P*<0.001.

phenotype is accompanied by a decrease in kinesin-1 associated with SCVs and the appearance at the cellular periphery of vesicles that are positive for PipB2 and kinesin-1 (Schroeder et al., 2010). This observation can be interpreted as a sign that SopD2 exerts an inhibitory activity on kinesin-1 linked to PipB2. It will be necessary to analyse the impact of these effectors and possibly others also present on SCVs to understand the regulation of kinesin-1 activity in the context of infection.

Kinesin-1 is an abundant molecular motor that is involved in a large number of transport processes in different cell types and cell sites (for reviews, see Dinu et al., 2007; Morfini et al., 2016; Verhey et al., 2001). Regulatory mechanisms for binding/detaching various cargoes are still poorly understood and the protein patterns recognized by KLCs for binding cargoes have only recently begun to be identified. A motif was originally found in the neural protein calsyntenin-1 (CSTN1, also known as CLSTN1) (Konecna et al., 2006). It consists of a peptide sequence containing a

tryptophan residue (W) flanked by negatively charged residues (D or E). This W-acidic motif has been identified in pathogen or host proteins. For example, it is duplicated in vaccinia virus protein A36 (Dodding et al., 2011), which is necessary for recruitment of kinesin-1 and transport of viral particles to the periphery of infected cells (Rietdorf et al., 2001). The same pattern is found in two copies in SKIP and is located in the N-terminal part of the protein while the interaction domain with SifA is in the C-terminal half (Boucrot et al., 2005; Pernigo et al., 2013). As no tryptophan residues are used in the composition of PipB2, the motif that allows this effector to interact with KLC must be different.

Several functional domains of PipB2 have been described. The N-terminal part (residues 1 to 225, out of a total of 350) is sufficient for translocation and localization on SCVs and tubules (Knodler et al., 2003), but not enough to cause the accumulation of LAMP1-positive vesicles at the cellular periphery, a phenotype observed upon overexpression of PipB2. This phenotype requires a
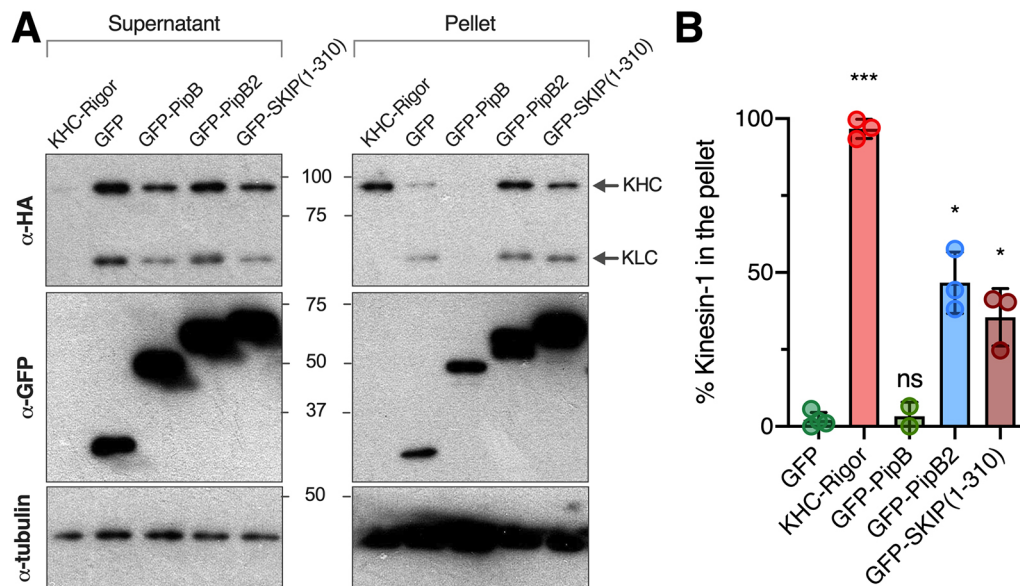
**Fig. 7. PipB2 activates kinesin-1 in the cellular context.** COS-7 cells were transfected with plasmids for the ectopic expression of HA-tagged KLC and KHC, and other proteins: GFP-PipB2, GFP and GFP-PipB (negative controls) or GFP-SKIP(1-310) (positive control). A HA-tagged ATPase 'rigor' mutant of KHC (KHC-R) was used as positive control for the experimental set-up. (A) Transfected cells were lysed under microtubule-stabilizing conditions, ultra-centrifuged on glycerol cushions, and the supernatants and pellets were analysed by western blotting for the presence of HA-tagged proteins (KLC, KHC and KHC-R), GFP-tagged proteins and tubulin. (B) Protein bands of western blots were quantified using ImageJ and the fraction of KHC present in the pellets was determined. Data are mean±s.d. of three independent experiments. A Dunnett's test was used to compare the fractions of activated kinesin-1 with those of the negative control (GFP). ns, $P>0.05$; *$P<0.05$; ***$P<0.001$.

pentapeptide, located in the last ten residues ($L_{341}FNEF_{345}$) (Knodler and Steele-Mortimer, 2005). It should be noted that this pentapeptide partially overlaps a sequence ($E_{344}FYSE_{348}$) that has the characteristics of a Y-acidic motif. The latter has recently been identified in the JIP1 protein and is, like the W-acidic motif, recognized by the KLC (Pernigo et al., 2018). However, the involvement of this sequence in the interaction between kinesin-1 and PipB2 is uncertain as the deletion of the pentapeptide, which partially covers this hypothesized Y-acidic motif, has only a partial effect on the interaction between PipB2 and KLC (Henry et al., 2006). All this information leads us to believe that, as already proposed (Knodler and Steele-Mortimer, 2005), other determinants of PipB2 that have not yet been identified are involved in the interaction with kinesin-1 and the regulation of its activity.

## MATERIALS AND METHODS
### Antibodies and reagents
The antibodies and reagents used in this study were: mouse anti-Myc (clone 9E10, homemade ascite, 1:1000), mouse anti-HA (clone 16B12, Covance, 1:1000), mouse anti-KLC (clone L1, Chemicon International, 1:50), mouse anti-β-tubulin (clone TUB 2.1, Sigma, 1:1000), mouse anti-histidine (clone HIS.H8; Thermo Fisher Scientific, 1:1000), rat anti-HA (clone 3F10; Roche Molecular Biochemicals, 1:500), goat anti-mouse or anti-rabbit IgG coupled to peroxidase (Sigma, 1:10,000), donkey anti-rat or anti-mouse IgG conjugated to Alexa Fluor 546 or Alexa Fluor 647 (Jackson ImmunoResearch, 1:500), HRP-conjugated streptavidin (Thermo Fisher Scientific, 1:10,000) and GFP-Trap (Chromotek). The rabbit anti-KHC (KIF5B, PCP42) was generously provided by R. Vale (University of California, San Francisco, CA, USA). Unless otherwise stated, all reagents were purchased from Sigma-Aldrich.

### Cell lines and culture conditions
HeLa (ATCC CCL-2) and COS-7 cells (ECACC General Cell Collection, 87021302) were routinely grown in Dulbecco's modified Eagle's medium (Gibco-BRL) supplemented with fetal calf serum 10% (Gibco-BRL) and glutamine 2 mM.

Hoxb8-immortalized macrophage-committed progenitor cells were derived from either wild-type C57BL/6 mouse or C57BL/6 not expressing KIF5B in hematopoietic cells following the procedure described by Redecke et al. (Redecke et al., 2013). In brief, bone marrow cells from the femurs were pre-stimulated for 48 h in RPMI 1640-based medium with 250 ng/ml SCF, 10 ng/ml IL3 and 20 ng/ml IL6. Ficoll-purified mononuclear cells were subjected to spinoculation with 1 ml of ER-Hoxb8 retrovirus. Infected progenitors were cultured in Progenitor Outgrowth Medium (RPMI 1640 with 10% FCS, 50 μM 2-mercaptoethanol, 2 mM glutamine, 1 μM β-oestradiol and 2% GM-CSF-conditioned medium from B16 melanoma expressing the Csf2 cDNA). Immortalized myeloid progenitors were selected by transferring nonadherent progenitor cells every 3 days to a new well in a six-well culture plate over 3 weeks to produce immortalized macrophage progenitor lines. Differentiation to macrophages was performed for 7 days in the same base medium free of β-oestradiol and GM-CSF but containing 10% M-CSF-conditioned medium from L929 cells.

### Bacterial strains, oligonucleotides and plasmids
A wild-type S. enterica serovar Typhimurium 12023 strain expressing SseJ-HA from the chromosome was transformed with pFPV25.1 (Valdivia and Falkow, 1996) for GFP expression. The ΔsifA mutant (AAG003G) was obtained by P22 transduction of ΔsifA::kan. The oligonucleotides and plasmids used in this study are described in Tables S1 and S2, respectively

### Bacterial infection of Hoxb8 macrophages and immunofluorescence
Hoxb8-immortalized cells were seeded in six-well plates with 12 mm diameter glass coverslips and differentiated for 7 days. Cells were Salmonella infected and processed for immunolabelling and fluorescence confocal microscopy as described previously (Zhao et al., 2016).

### Cloning, expression and purification
The pDEST17-Bio (V276) vector was obtained by modifying the pDEST17 Gateway destination vector by PCR to insert a biotin acceptor peptide (15-mer GLNDIFEAQKIEWHE) between the [His]6 tag and the attR1 site. Δ17PipB2 and SifAΔ6Bio were amplified by PCR from Salmonella 12023

wild-type genomic DNA using the primer pairs O786/O312 and O299/O806, respectively. The primer SifAΔ6BioRev was designed to add the biotin acceptor peptide sequence at the C-terminal. These PCR products were then inserted into pDONRZeo, resulting in the pDONR-Δ-17PipB2 (C1141) and pDONR-SifAΔ6-Bio (C1176). By recombination of pDONR-Δ17PipB2 with pDEST17-Bio and pDON-SifAΔ6-Bio with pDEST17, the final plasmids p[His]6-Bio-Δ17PipB2 (C1143) and p[His]6-SifAΔ-6Bio (C1177) were obtained. pWC2 (K401-Bio-H6) was a gift from Jeff Gelles (Addgene plasmid 15960) (Subramanian and Gelles, 2007).

Rosetta(DE3)pLysS competent cells (Novagen) containing pDEST17-SifAΔ6Bio or pWC2 (for the production of SifA-Bio or K401-Bio, respectively) were grown overnight at 25°C in MagicMedia E. coli expression medium (Thermo Fisher) supplemented with ampicillin 100 µg/ml and D-biotin 2.5 µg/ml. Rosetta containing pDEST17Bio-Δ17PipB2 (for the production of Bio-PipB2) was grown in 2× YT medium (Fisher Scientific) also supplemented with ampicillin and D-biotin. At OD600nm=0.8, overnight protein expression was induced by adding 0.5 mM IPTG at 25°C. Proteins were purified with Hi-Trap Chelating-Ni (GE Healthcare Life Sciences) on FPLC (ÄKTA Start, GE Healthcare Life Sciences) using a standard procedure. Finally, Bio-PipB2 was dialyzed against 50 mM imidazole (pH 6.7), 50 mM KCl, 4 mM MgCl$_2$, 2 mM EGTA, 10 mM β-mercaptoethanol and 20% glycerol. K401-Bio was dialyzed against the same buffer with 50 nM ATP. SifA-Bio was dialyzed as previously described (Diacovich et al., 2009). Proteins were snap-frozen in liquid N$_2$ and were stored at −80°C.

### MAP-depleted mouse brain cytosol preparation
Mouse brains were washed several times with PBS, homogenized in 1 ml/mg of lysis buffer [50 mM imidazole (pH 6.7), 1 mM MgCl$_2$, 2 mM EGTA, 1 µM DTT and 250 mM sucrose] and centrifuged at 10,000 $g$, 4°C, for 20 min. Proteinase inhibitors (Thermo Scientific) and 10 µM paclitaxel were added to the supernatant that was incubated for 30 min at 37°C. Finally, the sample was centrifuged at 107,000 $g$ for 30 min at 25°C (Optima MAX-XP; Beckman Coulter) and the supernatant was kept at −80°C.

### Fractionation of microtubule-based motor proteins
Mouse brains were homogenized in 1 ml/g PME [100 mM PIPES (pH 6.9), 2 mM EGTA, 1 mM MgSO$_4$, 1 mM DTT and 1 mM GTP]. The homogenate was centrifuged at 100,000 $g$ for 30 min at 4°C and the supernatant incubated for 30 min at 37°C with 2 units/ml apyrase and 20 µM paclitaxel, and for 30 extra minutes with 0.5 mM adenylyl-imidodiphosphate (AMP-PNP). After centrifugation at 39,000 $g$ for 30 min at 30°C, the pellet was resuspended in PME containing 0.1 mM AMP-PNP and 20 µM paclitaxel and centrifuged again. The pellet was resuspended in a small volume of PME with 20 µM paclitaxel and 10 mM Mg-ATP, incubated for 30 min at 37°C and centrifuged as in the previous steps. The supernatant was loaded on a linear sucrose gradient (5-20% in PME with 1 mM Mg-ATP), centrifuged at 31,500 rpm in a Beckman SW41 rotor for 16 h at 4°C and finally fractionated in aliquots of 0.5 ml that were stored at −80°C.

### Microtubule gliding assay
Polymerized microtubules were prepared by mixing Rhodamine-tubulin (Cytoskeleton) with purified porcine tubulin (Cytoskeleton) at a ratio of 1:100 in BRB80 buffer [80 mM PIPES (pH 6.7), 1 mM MgCl$_2$ and 1 mM EGTA] with 10% glycerol and 1 mM GTP and incubated at 37°C for 20 min, followed by addition of 10 µM paclitaxel and incubation for a further 20 minutes. Microtubules were kept room temperature and protected from light until use. The gliding assay was performed in a 10 µl flow chamber built with a glass slide, coverslip and parafilm spacers in between, joined by heating at 150°C for a few seconds. It was pre-coated with streptavidin (1 mg/ml) for 5 min and washed three times with wash buffer [BRB80 buffer (pH 6.7), 0.15 mg/ml casein, 5 mM DTT and 10 µM paclitaxel]. Protein buffer [10 µl of 20 mM Tris-HCl (pH 7.6), 300 mM NaCl, 10 mM β-mercaptoethanol, 2 mM EGTA and 20% glycerol] containing 20 µM K401-Bio, 5 µM Bio-PipB2 or 5 µM SifA-Bio were injected, incubated for 5 min and washed three times with the wash buffer. 10 µl of a kinesin-containing fraction was injected into the chambers containing Bio-PipB2 or SifA-Bio, incubated for 5 min and washed three

times with the wash buffer. 10 µl rhodamine-microtubules previously diluted 1:100 (0.01 mg/ml) in wash buffer were injected, incubated for 5 min and washed three times. Immediately before recording the microtubule movement, motility buffer [BRB80 buffer (pH 6.7), 0.15 mg/ml casein, 5 mM DTT, 10 µM paclitaxel, 0.18 mg/ml catalase, 0.37 mg/ml glucose oxidase, 10 mM glucose and 1 mM ATP] was introduced into the flow chamber and the chamber was sealed. Microtubules were observed using an epifluorescence microscope (Axio-observer; Zeiss) and time-lapse images (1 images/30 s) were captured for 2 to 30 min. Microtubule tracking was performed using FIJI (MTrackJ plugging, 100 microtubules per condition) and velocity of movement or quantification of bound microtubules was determined.

### Protein binding and membrane tube pulling from giant unilamellar vesicles
Giant unilamellar vesicles (GUVs) were prepared by electroformation (Angelova et al., 1992) with a lipid composition of 1,2-Dioleoyl-sn-Glycero-3-Phosphocholine 1 mM (DOPC; Avanti Polar Lipids) supplemented with 1% of BodipyFL-C5-HPC (Fisher Scientific) and 0.1% of the biotinylated lipid 1,2-Dioleoyl-sn-Glycero-3-Phosphoethanolamine-N-(Cap Biotinyl) (Biot-Cap-DOPE; Avanti Polar Lipids). 10 µl microtubules (1 mg/ml) in IMI buffer [50 mM imidazole (pH 6.7), 50 mM NaCl, 2 mM EGTA, 1 mM MgCl$_2$ and 10 µM paclitaxel] were injected into the chamber and incubated for 10 min before injecting 10 µl casein (7 mg/ml in IMI buffer). 10 µl of protein buffer with K401-Bio (20 µM) and streptavidin (7 µM) or 10 µl of kinesin-containing fraction with Bio-PipB2 (17 µM) or Bio-BSA (20 µM) and streptavidin (7 µM) were injected and incubated for 15 min. Finally, 10 µl of motility buffer [IMI buffer (pH 6.7), 5 mM DTT, 10 µM paclitaxel, 1 mM ATP, 0.18 mg/ml catalase, 0.37 mg/ml glucose oxidase and 10 mM glucose] and GUVs (1:10 v/v) were sequentially injected. The chamber was sealed and kept at 45° from the horizontal for few minutes to enable GUVs to settle before microscopic observation.

### Microtubule-binding protein spin-down assay
10 µl MAP-depleted mouse brain cytosol, 1 µM Bio-PipB2 or 1 µM SifA-Bio, 10 µM paclitaxel and 0.5 mM AMP-PNP in BRB80 buffer (pH 7.2) (final volume of 50 µl) were incubated for 30 min at room temperature in the presence or absence of 5 µl microtubules (1 mg/ml). K401-Bio was used as positive control. Reaction mixes were then ultra-centrifuged through a glycerol cushion (BRB80 buffer, 60% glycerol and 10 µM paclitaxel) for 40 min at 100,000 $g$ at 25°C. Supernatant and pellet were kept and mixed/resuspended with Laemmli sample buffer, and 20 µl of each sample were analysed by SDS-PAGE and western blotting.

### Transfection of cells
HeLa and COS-7 cells were transfected using FuGENE 6 following the manufacturer's protocol.

### Co-immunoprecipitation of proteins expressed in HeLa cells
Transfected HeLa cells were washed with PBS, scraped with a rubber policeman, centrifuged for 5 min at 400 $g$ and resuspended in 400 µl lysis buffer [10 mM Tris-HCl (pH 7.5), 150 mM NaCl, 0.5 mM EDTA and 0.5% NP-40] supplemented with a protease inhibitor cocktail. After 30 min at 4°C, cell lysates were centrifuged at 20.000 $g$ for 10 min at 4°C. 10% of the lysates were boiled in Laemmli sample buffer. Immunoprecipitations were performed with GFP-Trap beads that contain a recombinant alpaca anti-GFP antibody covalently coupled to agarose beads following manufacturer's protocol. Immunoprecipitated proteins were analysed by SDS-PAGE and western blotting using an appropriate antibody.

### Streptavidin bead pull-down
Bio-PipB2 or SifA-Bio, or a combination of both proteins in a ratio 1:1, were incubated with streptavidin-agarose beads for 30 min at room temperature. As negative controls, the same protocol without any protein was performed. The beads were pelleted at 2000 $g$ for 2 min, incubated with 10 µM D-biotin and washed three times with BRB80 buffer. Then they were incubated with MAP-depleted mouse brain cytosol for 30 min at room temperature and

washed three times as previously described. Finally, beads were resuspended in Laemmli sample buffer and western blotting was performed to analyse the bound proteins.

## Statistical analyses
Statistical analyses were performed using Prism 6 software (GraphPad).

## References
**Abrahams, G. L., Müller, P. and Hensel, M.** (2006). Functional dissection of SseF, a type III effector protein involved in positioning the salmonella-containing vacuole. *Traffic* **7**, 950-965. doi:10.1111/j.1600-0854.2006.00454.x

**Angelova, M. I., Soléau, S., Méléard, P., Faucon, F. and Bothorel, P.** (1992). Preparation of giant vesicles by external AC electric fields. In *Kinetics and Applications* (ed. C. Helm, M. Lösche and H. Möhwald), pp. 127-131. Darmstadt: Steinkopff.

**Aussel, L., Zhao, W., Hébrard, M., Guilhon, A.-A., Viala, J. P. M., Henri, S., Chasson, L., Gorvel, J.-P., Barras, F. and Méresse, S.** (2011). Salmonella detoxifying enzymes are sufficient to cope with the host oxidative burst. *Mol. Microbiol.* **80**, 628-640. doi:10.1111/j.1365-2958.2011.07611.x

**Bayer-Santos, E., Durkin, C. H., Rigano, L. A., Kupz, A., Alix, E., Cerny, O., Jennings, E., Liu, M., Ryan, A. S., Lapaque, N. et al.** (2016). The salmonella effector SteD mediates MARCH8-dependent ubiquitination of MHC II molecules and inhibits T cell activation. *Cell Host Microbe* **20**, 584-595. doi:10.1016/j.chom.2016.10.007

**Blasius, T. L., Cai, D., Jih, G. T., Toret, C. P. and Verhey, K. J.** (2007). Two binding partners cooperate to activate the molecular motor Kinesin-1. *J. Cell Biol.* **176**, 11-17. doi:10.1083/jcb.200605099

**Boucrot, E., Beuzón, C. R., Holden, D. W., Gorvel, J.-P. and Méresse, S.** (2003). Salmonella typhimurium SifA effector protein requires its membrane-anchoring C-terminal hexapeptide for its biological function. *J. Biol. Chem.* **278**, 14196-14202. doi:10.1074/jbc.M207901200

**Boucrot, E., Henry, T., Borg, J.-P., Gorvel, J.-P. and Méresse, S.** (2005). The intracellular fate of Salmonella depends on the recruitment of kinesin. *Science* **308**, 1174-1178. doi:10.1126/science.1110225

**Cai, D., Hoppe, A. D., Swanson, J. A. and Verhey, K. J.** (2007). Kinesin-1 structural organization and conformational changes revealed by FRET stoichiometry in live cells. *J. Cell Biol.* **176**, 51-63. doi:10.1083/jcb.200605097

**Diacovich, L., Dumont, A., Lafitte, D., Soprano, E., Guilhon, A.-A., Bignon, C., Gorvel, J.-P., Bourne, Y. and Méresse, S.** (2009). Interaction between the SifA virulence factor and its host target SKIP is essential for Salmonella pathogenesis. *J. Biol. Chem.* **284**, 33151-33160. doi:10.1074/jbc.M109.034975

**Dinu, C. Z., Chrisey, D. B., Diez, S. and Howard, J.** (2007). Cellular motors for molecular manufacturing. *Anat. Rec. (Hoboken)* **290**, 1203-1212. doi:10.1002/ar.20599

**Dodding, M. P., Mitter, R., Humphries, A. C. and Way, M.** (2011). A kinesin-1 binding motif in vaccinia virus that is widespread throughout the human genome. *EMBO J.* **30**, 4523-4538. doi:10.1038/emboj.2011.326

**Drecktrah, D., Levine-Wilkinson, S., Dam, T., Winfree, S., Knodler, L. A., Schroer, T. A. and Steele-Mortimer, O.** (2008). Dynamic behavior of Salmonella-induced membrane tubules in epithelial cells. *Traffic* **9**, 2117-2129. doi:10.1111/j.1600-0854.2008.00830.x

**Dumont, A., Boucrot, E., Drevensek, S., Daire, V., Gorvel, J.-P., Poüs, C., Holden, D. W. and Méresse, S.** (2010). SKIP, the host target of the Salmonella virulence factor SifA, promotes kinesin-1-dependent vacuolar membrane exchanges. *Traffic* **11**, 899-911. doi:10.1111/j.1600-0854.2010.01069.x

**Freeman, J. A., Ohl, M. E. and Miller, S. I.** (2003). The Salmonella enterica serovar typhimurium translocated effectors SseJ and SifB are targeted to the Salmonella-containing vacuole. *Infect. Immun.* **71**, 418-427. doi:10.1128/IAI.71.1.418-427.2003

**Gordon, M. A., Graham, S. M., Walsh, A. L., Wilson, L., Phiri, A., Molyneux, E., Zijlstra, E. E., Heyderman, R. S., Hart, C. A. and Molyneux, M. E.** (2008). Epidemics of invasive Salmonella enterica serovar enteritidis and S. enterica Serovar typhimurium infection associated with multidrug resistance among adults and children in Malawi. *Clin. Infect. Dis.* **46**, 963-969. doi:10.1086/529146

**Grummt, M., Pistor, S., Lottspeich, F. and Schliwa, M.** (1998). Cloning and functional expression of a "fast" fungal kinesin. *FEBS Lett.* **427**, 79-84. doi:10.1016/S0014-5793(98)00399-8

**Guardia, C. M., Farías, G. G., Jia, R., Pu, J. and Bonifacino, J. S.** (2016). BORC functions upstream of kinesins 1 and 3 to coordinate regional movement of lysosomes along different microtubule tracks. *Cell Rep.* **17**, 1950-1961. doi:10.1016/j.celrep.2016.10.062

**Henry, T., Couillault, C., Rockenfeller, P., Boucrot, E., Dumont, A., Schroeder, N., Hermant, A., Knodler, L. A., Lecine, P., Steele-Mortimer, O. et al.** (2006). The Salmonella effector protein PipB2 is a linker for kinesin-1. *Proc. Natl. Acad. Sci. USA* **103**, 13497-13502. doi:10.1073/pnas.0605443103

**Hirokawa, N. and Noda, Y.** (2008). Intracellular transport and kinesin superfamily proteins, KIFs: structure, function, and dynamics. *Physiol. Rev.* **88**, 1089-1118. doi:10.1152/physrev.00023.2007

**Knodler, L. A. and Steele-Mortimer, O.** (2005). The Salmonella effector PipB2 affects late endosome/lysosome distribution to mediate Sif extension. *Mol. Biol. Cell* **16**, 4108-4123. doi:10.1091/mbc.e05-04-0367

**Knodler, L. A., Vallance, B. A., Hensel, M., Jäckel, D., Finlay, B. B. and Steele-Mortimer, O.** (2003). Salmonella type III effectors PipB and PipB2 are targeted to detergent-resistant microdomains on internal host cell membranes. *Mol. Microbiol.* **49**, 685-704. doi:10.1046/j.1365-2958.2003.03598.x

**Knodler, L. A., Vallance, B. A., Celli, J., Winfree, S., Hansen, B., Montero, M. and Steele-Mortimer, O.** (2010). Dissemination of invasive Salmonella via bacterial-induced extrusion of mucosal epithelia. *Proc. Natl. Acad. Sci. USA* **107**, 17733-17738. doi:10.1073/pnas.1006098107

**Konecna, A., Frischknecht, R., Kinter, J., Ludwig, A., Steuble, M., Meskenaite, V., Indermühle, M., Engel, M., Cen, C., Mateos, J.-M. et al.** (2006). Calsyntenin-1 docks vesicular cargo to kinesin-1. *Mol. Biol. Cell* **17**, 3651-3663. doi:10.1091/mbc.e06-02-0112

**Krieger, V., Liebl, D., Zhang, Y., Rajashekar, R., Chlanda, P., Giesker, K., Chikkaballi, D. and Hensel, M.** (2014). Reorganization of the endosomal system in Salmonella-infected cells: the ultrastructure of Salmonella-induced tubular compartments. *PLoS Pathog.* **10**, e1004374. doi:10.1371/journal.ppat.1004374

**LaRock, D. L., Chaudhary, A. and Miller, S. I.** (2015). Salmonellae interactions with host processes. *Nat. Rev. Microbiol.* **13**, 191-205. doi:10.1038/nrmicro3420

**Leduc, C., Campàs, O., Zeldovich, K. B., Roux, A., Jolimaitre, P., Bourel-Bonnet, L., Goud, B., Joanny, J.-F., Bassereau, P. and Prost, J.** (2004). Cooperative extraction of membrane nanotubes by molecular motors. *Proc. Natl. Acad. Sci. USA* **101**, 17096-17101. doi:10.1073/pnas.0406598101

**Lelouard, H., Fallet, M., de Bovis, B., Méresse, S. and Gorvel, J.-P.** (2012). Peyer's patch dendritic cells sample antigens by extending dendrites through M cell-specific transcellular pores. *Gastroenterology* **142**, 592-601.e3. doi:10.1053/j.gastro.2011.11.039

**Leone, P. and Méresse, S.** (2011). Kinesin regulation by Salmonella. *Virulence* **2**, 63-66. doi:10.4161/viru.2.1.14603

**Liss, V., Swart, A. L., Kehl, A., Hermanns, N., Zhang, Y., Chikkaballi, D., Böhles, N., Deiwick, J. and Hensel, M.** (2017). Salmonella enterica remodels the host cell endosomal system for efficient intravacuolar nutrition. *Cell Host Microbe* **21**, 390-402. doi:10.1016/j.chom.2017.02.005

**Mazurkiewicz, P., Thomas, J., Thompson, J. A., Liu, M., Arbibe, L., Sansonetti, P. and Holden, D. W.** (2008). SpvC is a Salmonella effector with phosphothreonine lyase activity on host mitogen-activated protein kinases. *Mol. Microbiol.* **67**, 1371-1383. doi:10.1111/j.1365-2958.2008.06134.x

**Méresse, S., Unsworth, K. E., Habermann, A., Griffiths, G., Fang, F., Martínez-Lorenzo, M. J., Waterman, S. R., Gorvel, J.-P. and Holden, D. W.** (2001). Remodelling of the actin cytoskeleton is essential for replication of intravacuolar Salmonella. *Cell. Microbiol.* **3**, 567-577. doi:10.1046/j.1462-5822.2001.00141.x

**Morfini, G., Schmidt, N., Weissmann, C., Pigino, G. and Kins, S.** (2016). Conventional kinesin: biochemical heterogeneity and functional implications in health and disease. *Brain Res. Bull.* **126**, 347-353. doi:10.1016/j.brainresbull.2016.06.009

**Munoz, I., Danelli, L., Claver, J., Goudin, N., Kurowska, M., Madera-Salcedo, I. K., Huang, J.-D., Fischer, A., González-Espinosa, C., de Saint Basile, G. et al.** (2016). Kinesin-1 controls mast cell degranulation and anaphylaxis through PI3K-dependent recruitment to the granular Slp3/Rab27b complex. *J. Cell Biol.* **215**, 203-216. doi:10.1083/jcb.201605073

**Noster, J., Chao, T.-C., Sander, N., Schulte, M., Reuter, T., Hansmeier, N. and Hensel, M.** (2019). Proteomics of intracellular Salmonella enterica reveals roles of Salmonella pathogenicity island 2 in metabolism and antioxidant defense. *PLoS Pathog..* **15**, e1007741. doi:10.1371/journal.ppat.1007741

**Ohlson, M. B., Fluhr, K., Birmingham, C. L., Brumell, J. H. and Miller, S. I.** (2005). SseJ deacylase activity by Salmonella enterica serovar Typhimurium promotes virulence in mice. *Infect. Immun.* **73**, 6249-6259. doi:10.1128/IAI.73.10.6249-6259.2005

**Ohlson, M. B., Huang, Z., Alto, N. M., Blanc, M.-P., Dixon, J. E., Chai, J. and Miller, S. I.** (2008). Structure and function of Salmonella SifA indicate that its interactions with SKIP, SseJ, and RhoA family GTPases induce endosomal tubulation. *Cell Host Microbe* **4**, 434-446. doi:10.1016/j.chom.2008.08.012

**Pernigo, S., Lamprecht, A., Steiner, R. A. and Dodding, M. P.** (2013). Structural basis for kinesin-1: cargo recognition. *Science* **340**, 356-359. doi:10.1126/science.1234264

**Pernigo, S., Chegkazi, M. S., Yip, Y. Y., Treacy, C., Glorani, G., Hansen, K., Politis, A., Bui, S., Dodding, M. P. and Steiner, R. A.** (2018). Structural basis for isoform-specific kinesin-1 recognition of Y-acidic cargo adaptors. *Elife* **7**, 3439. doi:10.7554/eLife.38362

**Rajashekar, R., Liebl, D., Seitz, A. and Hensel, M.** (2008). Dynamic remodeling of the endosomal system during formation of Salmonella-induced filaments by intracellular Salmonella enterica. *Traffic* **9**, 2100-2116. doi:10.1111/j.1600-0854.2008.00821.x

**Redecke, V., Wu, R., Zhou, J., Finkelstein, D., Chaturvedi, V., High, A. A. and Häcker, H.** (2013). Hematopoietic progenitor cell lines with myeloid and lymphoid potential. *Nat. Meth* **10**, 795-803. doi:10.1038/nmeth.2510

**Rietdorf, J., Ploubidou, A., Reckmann, I., Holmström, A., Frischknecht, F., Zettl, M., Zimmermann, T. and Way, M.** (2001). Kinesin-dependent movement on microtubules precedes actin-based motility of vaccinia virus. *Nat. Cell Biol.* **3**, 992-1000. doi:10.1038/ncb1101-992

**Roux, A., Cappello, G., Cartaud, J., Prost, J., Goud, B. and Bassereau, P.** (2002). A minimal system allowing tubulation with molecular motors pulling on giant liposomes. *Proc. Natl. Acad. Sci. USA* **99**, 5394-5399. doi:10.1073/pnas.082107299

**Sanger, A., Yip, Y. Y., Randall, T. S., Pernigo, S., Steiner, R. A. and Dodding, M. P.** (2017). SKIP controls lysosome positioning using a composite kinesin-1 heavy and light chain-binding domain. *J. Cell Sci.* **130**, 1637-1651. doi:10.1242/jcs.198267

**Schroeder, N., Henry, T., de Chastellier, C., Zhao, W., Guilhon, A.-A., Gorvel, J.-P. and Méresse, S.** (2010). The virulence protein SopD2 regulates membrane dynamics of Salmonella-containing vacuoles. *PLoS Pathog.* **6**, e1001002. doi:10.1371/journal.ppat.1001002

**Schroeder, N., Mota, L. J. and Méresse, S.** (2011). Salmonella-induced tubular networks. *Trends Microbiol.* **19**, 268-277. doi:10.1016/j.tim.2011.01.006

**Stein, M. A., Leung, K. Y., Zwick, M., Portillo, F. G. and Finlay, B. B.** (1996). Identification of a Salmonella virulence gene required for formation of filamentous structures containing lysosomal membrane glycoproteins within epithelial cells. *Mol. Microbiol.* **20**, 151-164. doi:10.1111/j.1365-2958.1996.tb02497.x

**Subramanian, R. and Gelles, J.** (2007). Two distinct modes of processive kinesin movement in mixtures of ATP and AMP-PNP. *J. Gen. Physiol.* **130**, 445-455. doi:10.1085/jgp.200709866

**Valdivia, R. H. and Falkow, S.** (1996). Bacterial genetics by flow cytometry: rapid isolation of Salmonella typhimurium acid-inducible promoters by differential fluorescence induction. *Mol. Microbiol.* **22**, 367-378. doi:10.1046/j.1365-2958.1996.00120.x

**Verhey, K. J., Meyer, D., Deehan, R., Blenis, J., Schnapp, B. J., Rapoport, T. A. and Margolis, B.** (2001). Cargo of kinesin identified as JIP scaffolding proteins and associated signaling molecules. *J. Cell Biol.* **152**, 959-970. doi:10.1083/jcb.152.5.959

**Wang, G. G., Calvo, K. R., Pasillas, M. P., Sykes, D. B., Häcker, H. and Kamps, M. P.** (2006). Quantitative production of macrophages or neutrophils ex vivo using conditional Hoxb8. *Nat. Meth.* **3**, 287-293. doi:10.1038/nmeth865

**Zhao, W., Moest, T., Zhao, Y., Guilhon, A.-A., Buffat, C., Gorvel, J.-P. and Méresse, S.** (2015). The Salmonella effector protein SifA plays a dual role in virulence. *Sci. Rep.* **5**, 12979. doi:10.1038/srep12979

**Zhao, Y., Gorvel, J.-P. and Méresse, S.** (2016). Effector proteins support the asymmetric apportioning of Salmonella during cytokinesis. *Virulence* **7**, 669-678. doi:10.1080/21505594.2016.1173298